



Superhydrophilic–Superhydrophobic Template: A Simple Approach to Micro- and Nanostructure Patterning of TiO₂ Films

Yuekun Lai,^{a,b,z} Jianying Huang,^c Jiaojiao Gong,^a Yongxia Huang,^a
Chenglin Wang,^a Zhong Chen,^b and Changjian Lin^{a,*}

^aState Key Laboratory of Physical Chemistry of Solid Surfaces, and College of Chemistry and Chemical Engineering, Xiamen University, Xiamen 361005, People's Republic of China

^bSchool of Materials Science and Engineering, Nanyang Technological University, Singapore 639798

^cFujian Institute of Research on the Structure of Matter, Chinese Academy of Sciences, Fuzhou 350002, People's Republic of China

Vertically aligned TiO₂ nanotube (VATN) array micropatterns were fabricated based on a versatile superhydrophilic–superhydrophobic template. Scanning electron microscopy, optical microscopy, and an electron probe microanalyzer were systematically used to confirm the successful fabrication of the dual-scale (micro-/nanoscale) patterns and characterize their structure and morphology. The fabrication of the VATN patterning employed a simple photocatalytic lithography technique and mild reaction conditions at low temperature in the absence of a photoresist and a harmful chemical catalyst. This large-area dual-scale pattern based on the superhydrophilic–superhydrophobic template is expected to be a promising candidate for many applications in a broad range of scientific and technological areas, such as sensor arrays and optoelectronic devices.

© 2009 The Electrochemical Society. [DOI: 10.1149/1.3216032] All rights reserved.

Manuscript submitted March 30, 2009; revised manuscript received August 5, 2009. Published September 14, 2009.

The wettability of a solid surface is an important property that is governed by both its chemical compositions and geometrical structures.^{1–3} Superhydrophobicity with a water contact angle (CA) greater than 150° and superhydrophilicity with a CA below 5° are the two extreme cases and have attracted great interest due to their importance in fundamental research and practical application.^{4–8} Fine surface roughness enhances the modest hydrophilicity and hydrophobicity to superhydrophilicity and superhydrophobicity, respectively. At present, compared to the fabrications and applications based on the modest hydrophilic–hydrophobic pattern,^{9–13} there have been few reports on superhydrophilic–superhydrophobic patterning.^{14,15}

TiO₂, a wide bandgap functional semiconductor with numerous applications in sensing,^{16,17} optoelectronics,^{18,19} and photocatalysts,^{20,21} was chosen as the model system. Patterning TiO₂ nanostructures is particularly important in making new types of functional semiconductor devices and constructing micro- and nanoelectromechanical systems. Photolithography is the most powerful and successful technique for generating patterned structures over large areas. For the production of TiO₂ patterns, conventional photolithographic methods usually require polymer photoresists. However, it is difficult to find suitable etching conditions free of influence on the substrates at selective etching or to obtain high resolution pattern edges even after tearing the films during the lift-off process. To solve these problems, selective growth techniques have recently been developed.^{22–24} For example, Masuda et al. reported the site-selective deposition of anatase TiO₂ in an aqueous solution using a seed layer.²² Michel et al. reported a TiO₂ pattern built by the combination of selective wet etching and the reactive ion etching method.²³ However, these approaches have drawbacks in practical applications because of the need for expensive equipment, multiple complex steps, the use of resists, and the binding of a harmful metal catalyst, which greatly limit their utility in fabricating large areas of nanosize structures in a high throughput fashion. Therefore, the extension of a simple, low cost photolithographic method that does not require vacuum technology and photoresist/catalyst is highly promising.

In this work, we developed a simple photoresist-catalyst-free patterning process to create a fine TiO₂ nanostructured pattern with high resolution edges by wet chemical etching techniques. Large-scale superhydrophilic–superhydrophobic micropatterns with remarkable regularity were formed on a TiO₂ nanostructured surface

via electrochemical anodizing and UV locally photocatalytic lithography. This pattern, with an extreme wettability contrast, was then exploited as a template to guide the formation of vertical aligned titania nanotube (VATN) patterning (i.e., directed wet etch or vapor-condensing etch). The combination of wettability patterning on electrochemical anodizing VATN layer and subsequent selective wet etching offers a means of patterning a microscopic VATN on a large scale. Our strategies, in contrast to other methods, offer several advantages including extraordinary flexibility (fabrication performed under ambient conditions), low cost, and no need for a harmful metal catalyst or seeding layer. Hence, this approach based on extreme wettability template is particularly useful and promising in fabricating several kinds of functional nanostructures on large scales.

Experimental

The VATN films were prepared with a simple electrochemical anodization of pure titanium sheets (99.5%) with a Pt counter electrode under different conditions. TiO₂ nanotube films with an average tube diameter of 80 nm and a thickness of 400 nm were achieved under 20 V in a 0.5 wt % HF electrolyte solution for 20 min, which is the same as that of the previously reported method.^{25–28} Arrays of 80 nm nanotube films with a thickness of 1.53 μm were obtained by anodizing at 20 V for 100 min in a buffered neutral electrolyte containing 0.5 wt % NaF and 1 M Na₂SO₄.^{29,30} The as-prepared amorphous TiO₂ nanotube films were calcined at 450°C for 2 h to form the anatase phase.

The process for the superhydrophilic–superhydrophobic patterns and subsequent wet chemical etching is shown in Fig. 1. First, the annealing VATN samples were treated with a methanol solution of hydrolyzed 1 wt % 1H,1H,2H,2H-perfluorooctyl-triethoxysilane (PTES, Degussa Co., Ltd.) for 1 h and were subsequently heated at 140°C for 1 h to achieve surfaces with superhydrophobic property. Second, the PTES self-assembled monolayer (SAM) modified layer was irradiated with UV light (maximum intensity at 365 nm, 100 mW cm⁻²) for 20 min through a photomask to locally photocatalytically cleave the hydrophobic fluoroalkyl chain of the PTES.³¹ After being patterned with PTES, the superhydrophilic–superhydrophobic TiO₂ nanotube film was immersed into a 50 mL 0.1 wt % HF etching solution for a certain time to remove the TiO₂ nanotube within the unprotected superhydrophilic regions. After etching, the samples were then rinsed in Milli-Q water, and a final rinse in ethanol was performed before the samples were dried in air.

The morphology and composition of the patterns were observed by a field-emission scanning electron microscope (JEOL 6340, Japan). The chemical element distribution was measured by an elec-

* Electrochemical Society Active Member.

^z E-mail: mhsong@xmu.edu.cn; cjlin@xmu.edu.cn

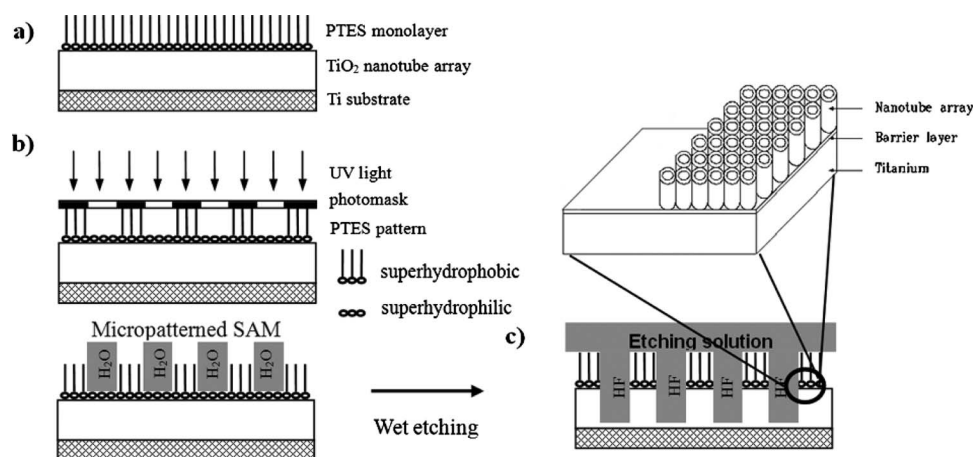


Figure 1. Schematic outline of the procedures in fabricating patterned TiO_2 nanotube arrays by wet etching based on the superhydrophilic–superhydrophobic template.

tron probe microanalyzer (EPMA, JEOL JXA-8100, Japan). For the fluorescence experiments, the obtained patterns were stained with a fluorescein sodium probe and observed by a Karl Zeiss fluorescence microscope (Axioskop2, MAT). The patterned TiO_2 nanotube array samples were observed by optical microscopy (Eclipse E600, Nikon).

Results and Discussion

The fabrication of superhydrophilic–superhydrophobic micropatterns on the VATN films is described in the Experimental section. Figure 2 shows the optical micrograph of the as-obtained superhydrophilic–superhydrophobic pattern by focusing on the droplet within the superhydrophilic regions. A uniform pattern is formed due to the site-selective wetting by water droplets within the superhydrophilic regions (Fig. 2a). A light dot array (inset of Fig. 2a) is seen when focusing on the top of the droplets, indicating that the confined droplet has a hemispherical dome. To further verify the resulting micropatterns with an extreme wettability contrast, fluorescein sodium was used as a probe to label the surface of the films. Figure 2b shows the fluorescent micrograph of the resultant superhydrophilic–superhydrophobic micropatterns on the VATN films. As shown, geometrically identical square superhydrophilic regions and dark superhydrophobic regions transferred well from the photomask to form a well-defined pattern. The UV-irradiated regions become superhydrophilic owing to the photocatalytic cleavage of the PTES molecule and the enhanced roughness of the nanotube structure, while the nonirradiated parts remain superhydrophobic without any change. Because the difference in the water CA between the irradiated and nonirradiated regions is larger than 150° , the liquid containing the fluorescent probe selectively appears only on the uniform superhydrophilic grids and not on the neighboring superhydrophobic regions. Therefore, a clear, well-defined fluorescent pat-

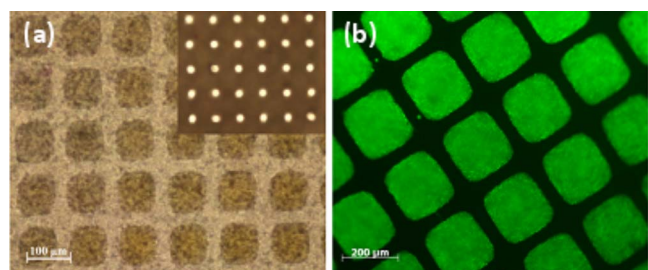


Figure 2. (Color online) (a) Optical micrograph of the as-obtained superhydrophilic–superhydrophobic pattern by focusing on the water droplet within the superhydrophilic regions. (b) Fluorescence microscopy image of the fluorescein probes on the as-prepared superhydrophilic–superhydrophobic micropattern.

tern in line with the dimensions of the Cu grid can be obtained. These results indicate that the micropatterned template composed of superhydrophilic and superhydrophobic regions was fabricated successfully.

The UV irradiation times had a great effect on the quality of the resulting pattern. For example, it cannot exhibit a sufficient wettability contrast between the irradiated and nonirradiated regions to form a well-defined pattern within 5 min. This is attributed to the hydrophobic fluoroalkyl chain in the PTES molecule that was not efficiently cleaved under a short-time UV irradiation. However, with a long-time UV irradiation (i.e., 60 min), the adjacent PTES molecule covered by the Cu grid can be remotely oxidized by a TiO_2 nanotube photocatalyst or the diffusion, scattering, and diffraction of the incident light.^{32,33} Therefore, to obtain a higher pattern resolution, the optimized UV irradiated time was controlled in the range of 10–30 min.

In previous work, PTES, as a material with low surface energy, could form close-packed SAMs on TiO_2 nanostructured surfaces to achieve superhydrophobicity.^{34,35} In addition, the PTES-SAMs on the VATN could achieve a superhydrophobic property to trap an air layer between the solid/liquid interface and could also be used as etching resists to effectively prevent the underlying layer from being etched under an aqueous corrosion environment,³⁶ which opens the possibility of using the wet chemical strategy to fabricate versatile functional nanostructure patterns. Based on this patterning template, we exploited the extreme wetting contrast between superhydrophilic grids and the adjacent superhydrophobic lines to direct the selectively wet etching of the VATN film in aqueous solution by a facile wet chemical etching technique.

The resulting TiO_2 nanotube micropatterns were observed using optical microscopy and scanning electron microscopy (SEM). Figure 3 shows an optical microscopy image of the TiO_2 nanotube micropattern produced using a grid micropattern with different wet etching times. A patterning with a clear outline was formed in a short time for 30 s (Fig. 3a). With an increase in the wet etching time (Fig. 3b and c), identical micropatterns with higher aspect ratios can be fabricated. When the etching was prolonged to 240 s (Fig. 3d), the size of the grids increased slightly, indicating that the PTES-SAM layer at the edge of the superhydrophobic lines is more easily etched as compared to the inner superhydrophobic area. This is due to the loose and disordered SAMs resulting from the scattered UV light photocatalytic degradation and the transfer of the active hydroxyl radicals at the edge of the grids. Moreover, the isotropic etching of the Ti substrate underneath the boundary leads to the collapse of the upper nanotube array structures. Therefore, the pattern can be obtained with a clear boundary in a short time after the wet etching in the aqueous solution, and the depth of the etching can be controlled simply by adjusting the etching time.

Figure 4 shows the detailed morphologies of the superhydrophilic regions with different etching times. The wet etching pro-

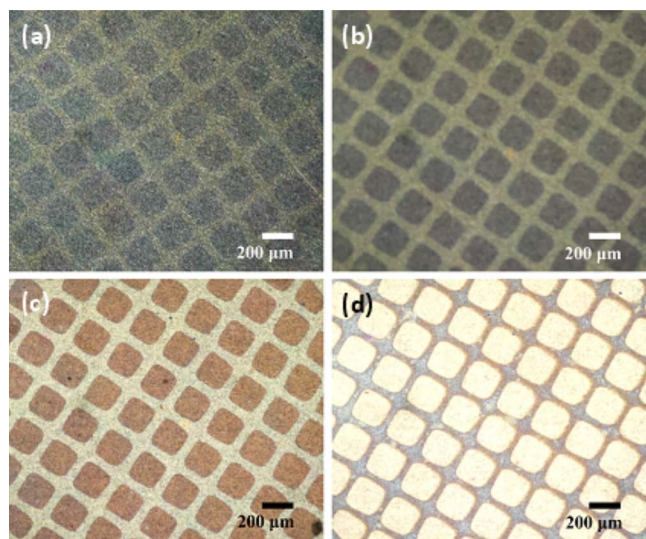


Figure 3. (Color online) Optical micrograph images of the time-resolved evolution process of the resulting VATN micropattern on a superhydrophilic–superhydrophobic template by wet chemical etching in 0.1 wt % HF solution: (a) 30, (b) 60, (c) 120, and (d) 240 s.

cesses are developed as expected for an isotropic etch, starting off as flat depressions and proceeding evenly in all directions, evolving toward hemispherical shapes while undermining the inside compact materials. However, the superhydrophilic TiO_2 nanotube regions were rapidly etched away except for the rough tube bottom layer with a thickness of about 40 nm in a short time of 30 s (Fig. 4a), indicating that the wet etching is preferential along the vertical TiO_2 nanotube direction. We supposed that the VATN structure could induce a faster etching for the perpendicular direction than that of the horizontal plane due to the capillary injection through the vertical tube channels. With increasing etching time, the continued tube bottom layer further changed to round isolated ones (Fig. 4b) and was completely removed to expose the compact barrier layer with concave dimples after 120 s (Fig. 4c). Etching for longer times (Fig. 4d) leads to the exposure of the smooth Ti substrate.

Representative SEM images of the TiO_2 nanotube array micropatterns by selective wet etching in 0.1 wt % HF solution for 120 s are shown in Fig. 5. The well-defined pattern consisted of Ti metal

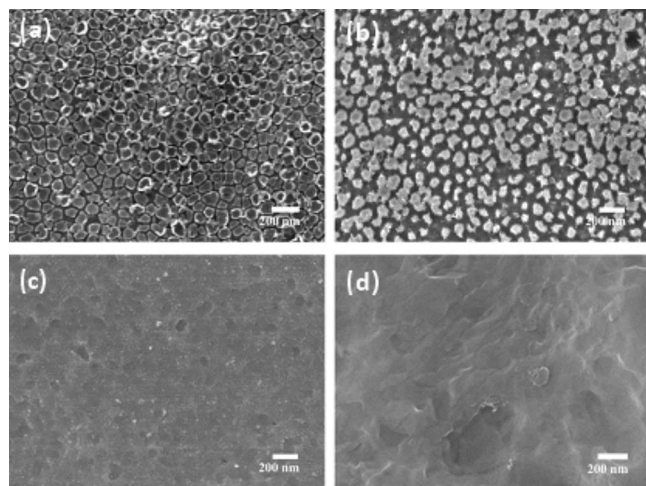


Figure 4. SEM images of the superhydrophilic regions corresponding to the optical micrographs of the patterning shown in Fig. 3a–d: (a) 30, (b) 60, (c) 120, and (d) 240 s.

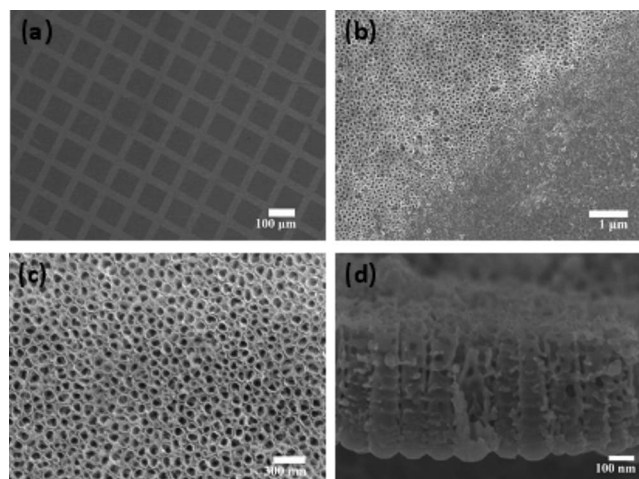


Figure 5. (a) SEM micrograph of the patterned TiO_2 nanostructured micro-patterns by wet chemical method, magnified image of the (b) superhydrophilic–superhydrophobic boundary, (c) superhydrophobic area, and (d) its cross-sectional image.

microgrids and TiO_2 nanotube array lines (Fig. 5a and b). In superhydrophilic regions (Fig. 4c), the smooth Ti metal substrate is clearly seen due to its upper rough TiO_2 nanotube array layer that is etched completely by the confined etchant. However, there are no apparent damages in the superhydrophobic region (Fig. 5c), which is protected by the PTES-SAM layer, and its indirect contact with the etchant due to a large amount of air was trapped between the nanotube array and the etchant.^{34,35} The tube diameter is about 80 nm while the etching depth is approximately 400 nm for 120 s (Fig. 5d). The aspect ratio of etching patterns is over 5:1. Due to the PTES layer thickness of less than 2 nm,^{37,38} the etching selectivity of the TiO_2 nanotube to the PTES resist is high at about 200. This is greatly due to the air trapped between the solid/liquid interface within the superhydrophobic regions and the capillary-induced quick etching along the vertical nanotube structure at the superhydrophilic regions.

The chemical composition changes in the corresponding micropattern were also further verified by an EPMA. The EPMA allows analysts to obtain a sufficiently high accuracy when determining the different chemical compositions of the pattern. Figure 6 shows the oxygen element distribution map and the corresponding line scan signal intensity profiles across the grid pattern (indicated by a dotted line) by wet chemical etching for 120 s. As shown in the map, large areas of order patterns (Fig. 6a) with clear boundaries were obtained as a result of the selective etching of TiO_2 nanostructures in aqueous solution. The line profiling (Fig. 6b) of the oxygen signal intensity decreased greatly, and the signal intensity of Ti changed only a little after the wet etching. This suggests that most or all of the TiO_2 nanotube layers in the homogeneous blue grid areas corresponding to the superhydrophilic regions were etched away, while the surrounding red line areas remained intact under the protection of the PTES-SAM layer. Due to the influence of the Ti substrate, the disparities of the Ti element intensity between the superhydrophilic and superhydrophobic regions are insufficient. This agrees well with the results observed by SEM. The slight deviation from the detected signal intensity is due to the analytical errors caused by the rough nanostructures.

The micropattern with a higher aspect ratio can also be fabricated by a developed wet chemical etching technique. The periodically superhydrophilic grids separated by mutually perpendicular superhydrophobic lines provided different wettabilities for the solution. As water evaporated, the vapor containing HF dewetted the superhydrophobic lines while condensing on the superhydrophilic grids to etch the VATN layer. This situation agrees with Fig. 2a and with the

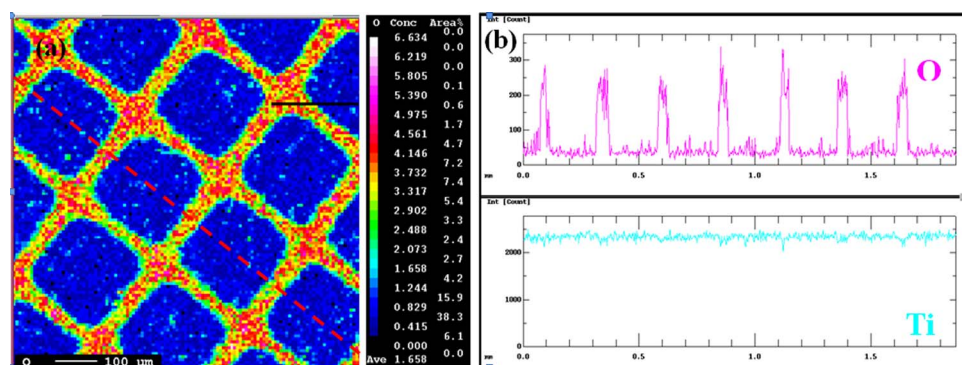


Figure 6. (Color online) (a) The area scanning chemical composition map of the as-prepared VATN micropattern by wet chemical etching in 0.1 wt % HF solution for 120 s. (b) The line-scan signal intensity measurements were performed across the superhydrophilic grids as indicated by a dotted line in the area-scan image of (a).

report by Wu et al.³⁹ Figure 7a and b shows the as-prepared TiO₂ micropattern with a clear boundary by water vapor etching for 10 min. This resulted from the selective condensing of the vapor from the water solution containing 5 wt % HF in the superhydrophilic regions. Some collapsed residue (indicated by the black arrow) covers the boundary due to the rapid etching of the bottom nanotubes and the resultant bubbles; however, they can be easily removed by sonication. The VATN structure film with a length of about 1.53 μm shows no obvious change within the superhydrophobic regions (Fig. 7c), while the TiO₂ nanotubes in the superhydrophilic regions are etched completely for 20 min (Fig. 7d), that is to say, a TiO₂ micropattern with a high aspect ratio of ~20 can be obtained. This technique is particularly attractive in generating large-area functional nanostructure patterns in a high throughput fashion with a high aspect ratio.

The advantages of our approach lie in its generality. Our assembly strategy can be easily extended to other vertical aligned nanostructured materials and microstructures of any arbitrary shape. In addition, such versatile assembly of functional nanomaterials based on superhydrophobic–superhydrophilic templates can open avenues to micro- and nanodevice fabrication and enable applications in a wide variety of fields such as microfluidic devices,⁴⁰ biotechnology,^{41,42} water harvesting surfaces⁴³ and site-selective deposition templates,^{44,45} etc.

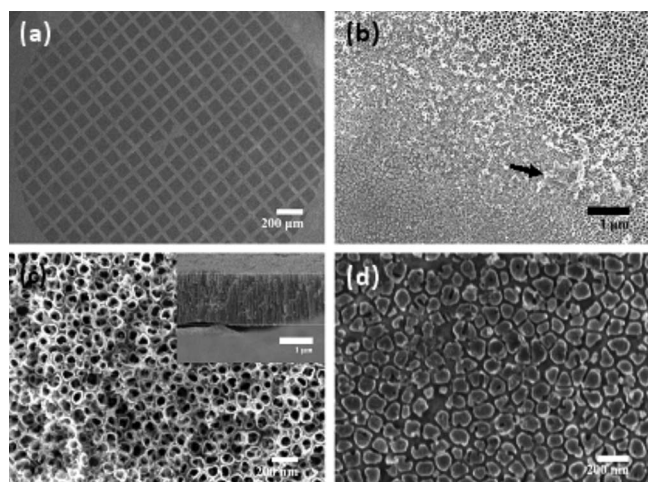


Figure 7. (a) The SEM micrograph of the ordered VATN array pattern by vapor-condense etching for 10 min. Magnified images of the corresponding (b) superhydrophilic–superhydrophobic boundary, (c) superhydrophobic area, and (d) superhydrophilic area. The inset figure shows the corresponding cross-sectional image.

Conclusions

In summary, we have demonstrated a simple synthesized approach based on wettability for the selective erase of a vertical TiO₂ nanotube array layer to form a dual-scale pattern directly in a liquid solution on a Ti substrate using a wet chemical method. This micro- and nanochemical patterning strategy can be expanded to other nanostructure materials with complex substrate shapes and has many potential applications in advanced technologies.

Acknowledgments

The authors thank the National Natural Science Foundation of China (grant no. 50571085 and no. 20620130427), the National Basic Research Program of China (973 Program no. 2007CB935603 and no. 2007DFC40440) for their financial support.

Xiamen University assisted in meeting the publication costs of this article.

References

1. R. Wang, K. Hashimoto, A. Fujishima, M. Chikuni, E. Kojima, A. Kitamura, M. Shimohigoshi, and T. Watanabe, *Nature (London)*, **388**, 431 (1997).
2. K. Ichimura, S. K. Oh, and M. Nakagawa, *Science*, **288**, 1624 (2000).
3. X. F. Gao and L. Jiang, *Nature (London)*, **432**, 36 (2004).
4. E. Balaur, J. M. Macak, L. Taveira, and P. Schmuki, *Electrochem. Commun.*, **7**, 1066 (2005).
5. X. Yu, Z. Q. Wang, Y. G. Jiang, F. Shi, and X. Zhang, *Adv. Mater. (Weinheim, Ger.)*, **17**, 1289 (2005).
6. P. Aussillous and D. Quéré, *Nature (London)*, **411**, 924 (2001).
7. L. Feng, S. Li, Y. Li, H. Li, L. Zhang, J. Zhai, Y. Song, B. Liu, L. Jiang, and D. B. Zhu, *Adv. Mater. (Weinheim, Ger.)*, **14**, 1857 (2002).
8. F. C. Cebeci, Z. Z. Wu, L. Zhai, R. E. Cohen, and M. F. Rubner, *Langmuir*, **22**, 2856 (2006).
9. Y. Gao, Y. Masuda, and K. Koumoto, *Chem. Mater.*, **16**, 1062 (2004).
10. Y. Masuda, N. Kinoshita, F. Sato, and K. Koumoto, *Cryst. Growth Des.*, **6**, 75 (2006).
11. K. Koumoto, N. Saito, Y. F. Gao, Y. Masuda, and P. X. Zhu, *Bull. Chem. Soc. Jpn.*, **81**, 1337 (2008).
12. T. Balgar, S. Franzka, E. Hasselbrink, and N. Hartmann, *Appl. Phys. A: Mater. Sci. Process.*, **82**, 15 (2006).
13. A. Matsuda, T. Sasaki, K. Tadanaga, M. Tatsumisago, and T. Minami, *Chem. Mater.*, **14**, 2693 (2002).
14. X. T. Zhang, O. Sato, and A. Fujishima, *Langmuir*, **20**, 6065 (2004).
15. K. Tadanaga, J. Morinaga, A. Matsuda, and T. Minami, *Chem. Mater.*, **12**, 590 (2000).
16. O. K. Varghese, D. Gong, M. Paulose, K. G. Ong, E. C. Dickey, and C. A. Grimes, *Adv. Mater. (Weinheim, Ger.)*, **15**, 624 (2003).
17. Y. Y. Zhang, W. Y. Fu, H. B. Yang, Q. Qi, Y. Zeng, T. Zhang, R. X. Ge, and G. Zou, *Appl. Surf. Sci.*, **254**, 5545 (2008).
18. S. H. Kang, J. Y. Kim, Y. Kim, H. S. Kim, and Y. E. Sun, *J. Phys. Chem. C*, **111**, 9614 (2007).
19. R. Vogel, P. Meredith, I. Kartini, M. Harvey, J. D. Riches, A. Bishop, N. Heckenberg, M. Trau, and H. Rubinsztein-Dunlop, *ChemPhysChem*, **4**, 595 (2003).
20. Y. K. Lai, L. Sun, Y. C. Chen, H. F. Zhuang, C. J. Lin, and J. W. Chin, *J. Electrochem. Soc.*, **153**, D123 (2006).
21. Z. Y. Liu, X. T. Zhang, S. Nishimoto, T. Murakami, and A. Fujishima, *Environ. Sci. Technol.*, **42**, 8547 (2008).
22. Y. Masuda, S. Ieda, and K. Koumoto, *Langmuir*, **19**, 4415 (2003).
23. R. Michel, J. W. Lussi, G. Csucs, I. Reviakine, G. Danuser, B. Ketterer, J. A. Hubbell, M. Textor, and N. D. Spencer, *Langmuir*, **18**, 3281 (2002).
24. P. Yang, M. Yang, S. L. Zou, J. Y. Xie, and W. T. Yang, *J. Am. Chem. Soc.*, **129**,

- 1541 (2007).
25. D. W. Gong, C. A. Grimes, and O. K. Varghese, *J. Mater. Res.*, **16**, 3331 (2001).
 26. L. V. Taveira, J. M. Macak, H. L. Tsuchiya, F. P. Dick, and P. Schmuki, *J. Electrochem. Soc.*, **152**, B405 (2005).
 27. A. Seyeux, S. Berger, D. LeClere, A. Valota, P. Skeldon, G. E. Thompson, J. Kunze, and P. Schmuki, *J. Electrochem. Soc.*, **156**, K17 (2009).
 28. Y. K. Lai, H. F. Zhuang, L. Sun, Z. Chen, and C. J. Lin, *Electrochim. Acta*, **54**, 6536 (2009).
 29. J. M. Macak, K. Sirotna, and P. Schmuki, *Electrochim. Acta*, **50**, 3679 (2005).
 30. L. V. Taveira, A. A. Saguees, J. M. Macak, and P. Schmuki, *J. Electrochem. Soc.*, **155**, C293 (2008).
 31. Y. K. Lai, C. J. Lin, H. Wang, J. Y. Huang, H. F. Zhuang, and L. Sun, *Electrochem. Commun.*, **10**, 387 (2008).
 32. H. Haick and Y. Paz, *J. Phys. Chem. B*, **105**, 3045 (2001).
 33. W. Kubo, T. Tatsuma, A. Fujishima, and H. Kobayashi, *J. Phys. Chem. B*, **108**, 3005 (2004).
 34. Y. K. Lai, C. J. Lin, J. Y. Huang, H. F. Zhuang, L. Sun, and T. Nguyen, *Langmuir*, **24**, 3867 (2008).
 35. Y. K. Lai, X. F. Gao, H. F. Zhuang, J. Y. Huang, C. J. Lin, and L. Jiang, *Adv. Mater. (Weinheim, Ger.)*, In press. [DOI: 10.1002/adma.200900686]
 36. H. Sugimura, T. Hanji, O. Takai, T. Masuda, and H. Misawa, *Electrochim. Acta*, **47**, 103 (2001).
 37. D. Schondelmaier, S. Cramm, R. Klingeler, J. Morenzin, Ch. Zilkens, and W. Eberhardt, *Langmuir*, **18**, 6242 (2002).
 38. J. D. J. S. Samuel and J. Rühle, *Langmuir*, **20**, 10080 (2004).
 39. Y. Y. Wu, M. Kouno, N. Saito, F. A. Nae, Y. Inoue, and O. Takai, *Thin Solid Films*, **515**, 4203 (2007).
 40. B. Zhao, J. S. Moore, and D. J. Beebe, *Science*, **291**, 1023 (2001).
 41. H. Sorribas, C. Padeste, and L. Tiefenauer, *Biomaterials*, **23**, 893 (2002).
 42. Y. Ito, *Biomaterials*, **20**, 2333 (1999).
 43. L. Zhai, M. C. Berg, F. C. Cebeci, Y. Kim, J. M. Milwid, M. F. Rubner, and R. E. Cohen, *Nano Lett.*, **6**, 1213 (2006).
 44. T. Ishizaki, H. Sakurai, N. Saito, and O. Takai, *Surf. Coat. Technol.*, **202**, 5535 (2008).
 45. N. Shirahata and A. Hozumi, *Chem. Mater.*, **17**, 20 (2005).